## Supplemental data:

# Synaptic SAP97 Isoforms Regulate AMPA Receptor Dynamics and Access to Presynaptic Glutamate

Clarissa L. Waites, Christian G. Specht, Kai Härtel, Sergio Leal-Ortiz, Dong Li, Renaldo C. Drisdel, Okun Jeyifous, David Genoux, Juliette E. Cheyne, William N. Green, Johanna M. Montgomery, Craig C. Garner

## Results

Expression levels of α– and βSAP97 isoforms in hippocampal neurons

To estimate the expression levels of recombinant α– or βSAP97-EGFP in hippocampal neurons relative to endogenous SAP97, we analyzed lysates of neurons infected at high titer (~90% infection rate) with α– or βSAP97-EGFP by Western blot. Probing with SAP97 antibodies allowed us to visualize total levels of endogenous SAP97 as well as those of the overexpressed α– and β-isoforms (Fig. S1A). This revealed that α– and βSAP97-EGFP appear to be overexpressed ~2-3 fold relative to endogenous SAP97 in total cellular lysates. Further, overexpression of α– and βSAP97-EGFP does not appear to affect the expression of endogenous SAP97.

We also estimated the degree of α– and βSAP97-EGFP overexpression in spines of neurons transfected using calcium phosphate precipitation, the method used for the electrophysiological experiments and in the study of endogenous surface GluR1 and mCh-GluR1 localization and dynamics. Since this transfection method is far less efficient (<5% of transfected cells), we could not use Western blotting for analysis. Similarly, immunostaining with SAP97 antibodies was not possible, as these antibodies are of insufficient quality for immunocytochemistry in dissociated hippocampal neurons. Further, endogenous SAP97 levels in spines of hippocampal neurons are low relative to other postsynaptic MAGUK proteins, such as PSD-95 (Schlüter *et al.* 2006), suggesting that PSD-95 typically has a dominant role in regulating

synaptic AMPARs in the hippocampus. However, when expressed at comparable levels, SAP97 isoforms could exert a greater influence, enabling their roles in synaptic AMPAR trafficking to be ascertained. Thus, we decided to quantify the degree of SAP97-EGFP overexpression relative to endogenous PSD-95 levels in dendritic spines.

For this analysis, we first compared the expression levels of endogenous and EGFP-tagged PSD-95 using PSD-95 antibodies. By immunostaining, we found no difference in the intensity of PSD-95 puncta in untransfected neurons relative to those transfected with PSD-95-EGFP (Fig. S1B, left column). This result suggests that our transfection method is capable of expressing this protein at near-endogenous levels, and that endogenous PSD-95 expression is downregulated in transfected neurons. Subsequently, using identical settings for image acquisition, a direct comparison of EGFP intensity in spines of neurons transfected with αSAP97-EGFP or βSAP97-EGFP revealed only modest overexpression of the two SAP97 isoforms by ~1.5 fold and ~2 fold, respectively, relative to the level of PSD-95-EGFP (Fig. S1B, right column). Clearly, these data represent estimates, as we typically observe cell-to-cell variability in protein expression levels, as well as higher levels of synaptic αSAP97-EGFP expression relative to βSAP97-EGFP. Nevertheless, our findings demonstrate that the degree of SAP97-EGFP overexpression in calcium phosphate-transfected neurons is modest and comparable to that of endogenous PSD-95. Furthermore, the comparison of spine intensity values of α- and βSAP97-EGFP at synapses from neurons infected with lentivirus (Fig. S2A) or transfected neurons (Fig. S6A) reveal that these levels of expression are comparable.

Subsynaptic localization of α– and βSAP97-EGFP

To examine the subsynaptic distributions of α– and βSAP97, we optimized an existing protocol utilizing silver-enhanced immunogold EM to label EGFP-tagged proteins in dissociated hippocampal neurons (Micheva *et al.* 2003). As depicted in Figure S4B, the two most commonly observed sites for βSAP97-EGFP labeling were near the spine plasma membrane, typically peripheral to the PSD, or within the spine head. Since we did not perform serial sectioning, we could not discern whether labeling within the spine head also represented plasma membrane-associated protein in a different z-axis, or intracellular cytoplasmic or membrane-associated protein. We also observed βSAP97-EGFP labeling at the PSD (Fig. S4B, bottom right panel). However, compared to αSAP97-EGFP, which consistently and intensely labeled the entire length

of the PSD (Fig. S4A), βSAP97-EGFP appeared to label only sub-domains of this structure. Together with the rest of our data, these images indicate that α- and β-isoforms have fundamentally distinct localizations within dendritic spines, with αSAP97 primarily associated with the PSD and βSAP97 with non-PSD structures, including the peripheral plasma membrane and intracellular regions. In addition, labeling for both proteins was occasionally observed in presynaptic boutons, sometimes associated with synaptic vesicles (as seen for βSAP97 in Fig. S4B, lower right).

Specificity of interaction between SAP97 and GluR1

To confirm binding between the SAP97-EGFP constructs and GluR1, we coexpressed mCh-GluR1 with α–, β– or ΔSAP97-EGFP in HEK cells, harvested cellular lysates, and immunoprecipitated mCh-GluR1 from these lysates using polyclonal RFP antibodies (which also recognize mCherry). As shown in Figure S5B, all SAP97-EGFP constructs were pulled down with anti-RFP but not anti-IgG antibody, confirming a specific interaction between SAP97-EGFP and mCh-GluR1. Furthermore, this interaction was not affected by deletion of the N-terminus of SAP97, in agreement with previous reports showing that binding is governed by the distal C-terminal PDZ domain (Leonard *et al.* 1998, Cai *et al.* 2002).

As an additional test for the specificity of the SAP97-GluR1 interaction, we examined whether α- or βSAP97-EGFP promoted the accumulation of the GluR3 subunit of AMPARs within dendritic spines of dissociated hippocampal neurons. Since this subunit does not form heterotetramers with GluR1 (only GluR1/2 or GluR2/3 complexes exist in hippocampal neurons), and has never been shown to bind SAP97, it should not be influenced by either GluR1 or SAP97 localization. Indeed, we did not observe any postsynaptic accumulation of GluR3 in spines of neurons overexpressing α– or βSAP97-EGFP (Fig. S5C), demonstrating the specificity of SAP97-GluR1 binding.

Transsynaptic effects of postsynaptic α– and βSAP97-EGFP expression

Our previous study showed that postsynaptic βSAP97 overexpression caused an increase in the size of adjacent presynaptic boutons via transsynaptic signaling (Regalado *et al.* 2006). Since changes in presynaptic function could potentially contribute to the electrophysiological differences seen in neurons expressing α– or βSAP97-EGFP, we decided to compare the effects

of postsynaptic α- and βSAP97 overexpression on presynaptic size and function. We used FM4-64 uptake and destaining to assess the sizes and exocytosis rates, respectively, of the total recycling pool (TRP) of synaptic vesicles (SVs) in boutons adjacent to SAP97-expressing postsynaptic sites. First, coverslips containing neurons transfected with α–, β– or ΔSAP97-EGFP were mounted on a confocal microscope and loaded with FM4-64 (90 mM KCl, 60 sec) to label the TRP of SVs. After acquiring images from at least 8 fields of view (containing 1-2 transfected and a similar number of untransfected neurons) for each construct, we used custom software (OpenView, N. Ziv) to compare the fluorescence intensities of FM4-64 puncta adjacent to α–, β–, or ΔSAP97-transfected neurons with those adjacent to untransfected neurons in the same field of view (see Fig. S8A). We found that α– and βSAP97-EGFP had significant (t test, $p<0.0005$ for both α– and βSAP97) and nearly identical transsynaptic effects on the TRP size of adjacent boutons, increasing their intensities by an average of ~35% compared to control cells (αSAP97 = 37% +/- 5%, βSAP97 = 33% +/- 6%)(Fig. S8A-C). In contrast, ΔSAP97-EGFP had no effect on the TRP size of adjacent boutons (average intensity increase of 1% +/- 4% compared to control boutons), consistent with its inability to become stably anchored within postsynaptic spines or to recruit other transmembrane proteins, such as GluR1, to these sites.

These results demonstrate that α– and βSAP97 may enhance the ability of SVs at adjacent presynaptic boutons to undergo exocytosis. To examine this effect more closely, we compared the FM destaining rates of boutons adjacent to α- and βSAP97-expressing spines and control boutons. Here, α– and βSAP97-EGFP transfected cultures were mounted on the confocal microscope and the TRP of vesicles labeled with FM4-64 as described above. Images were acquired before and every 5 sec during a 10 Hz, 90 sec stimulus train. Following stimulation, boutons were destained completely with 90 mM KCl (60 sec) to obtain measurements of background FM4-64 fluorescence. To obtain destaining curves, we used OpenView software to measure the FM4-64 fluorescence intensity (F) of the puncta at each timepoint ($t$) relative to the initial fluorescence intensity prior to destaining, and normalized these values to FM background fluorescence ($F_b$) using the following equation: $((F_t / F_{t=0}) - F_b) / (1 - F_b)$. Individual puncta were averaged for a given condition and field of view, and the resulting curves averaged to give the final destaining curves. We found that α– and βSAP97 expression resulted in similar FM destaining rates, with boutons adjacent to transfected spines having only marginally faster destaining rates than those adjacent to untransfected spines (Fig. S8D,E). These results indicate

that both α– and βSAP97 increased the size of the TRP of SVs to a similar extent, without significantly altering the kinetics of SV release. Thus, differential effects of α– and βSAP97 on presynaptic function are unlikely to account for the dramatic differences seen in AMPAR EPSC amplitudes for neurons expressing α– or βSAP97.

## References

Cai C, Coleman SK, Niemi K, Keinanen K (2002) Selective binding of synapse-associated protein 97 to GluR-A alpha-amino-5-hydroxy-3-methyl-4-isoxazole propionate receptor subunit is determined by a novel sequence motif. J Biol Chem 277:31484-31490.

Leonard AS, Davare MA, Horne MC, Garner CC, Hell JW (1998) SAP97 is associated with the alpha-amino-3-hydroxy-5-methylisoxazole-4-propionic acid receptor GluR1 subunit. J Biol Chem 273:19518-19524.

Micheva KD, Buchanan J, Holz RW, Smith SJ (2003) Retrograde regulation of synaptic vesicle endocytosis and recycling. Nat Neurosci 6:925-932.

Regalado MP, Terry-Lorenzo RT, Waites CL, Garner CC, Malenka RC (2006) Transsynaptic signaling by postsynaptic synapse-associated protein 97. J Neurosci 26:2343-2357.

Schlüter OM, Xu W, Malenka RC (2006) Alternative N-terminal domains of PSD-95 and SAP97 govern activity-dependent regulation of synaptic AMPA receptor function. Neuron 51:99-111.

## Methods

Lentivirus Production

HEK cells were grown to confluence in DMEM medium containing 10% FBS and the medium was exchanged for Neurobasal medium containing GlutaMAX and B27 prior to transfection. Cells were cotransfected with pFUGW constructs (10 μg) together with the helper plasmids Δ8.9 (7.5 μg) and VSVg (5 μg) in 1.5 ml Opti-MEM medium (Invitrogen), using 60 μl lipofectamine 2000 (Invitrogen) according to the supplier's protocol. HEK cells were then incubated at 32°C / 5% $CO_2$. The medium was exchanged and discarded after 24 h and the virus was harvested with the culture medium after ~55 h and stored as aliquots at –80°C. Lentivirus titers were generally in the range of $10^8$/ml, as judged by counting EGFP-fluorescent HEK cells.

Palmitoylation Assay

HEK cells expressing α–, β– or ΔSAP97 were solubilized in 1% Triton X-100 supplemented with protease inhibitors and 20 mM NEM. Immunoaffinity-purified protein bound to protein G-Sepharose was washed once in lysis buffer without Triton but containing 0.1% SDS, 0.5 M NaCl, 20 mM NEM followed by three washes in normal lysis buffer without NEM and treated with 1 M hydroxylamine, pH 7.4, for 1 h at room temperature. Controls were incubated in the presence of 1 M Tris, pH 7.4. The beads were washed twice with lysis buffer. Samples were labeled with 0.5 mM Btn-BMCC (1-biotinamido-4-[4'-(maleididomethyl) cyclohexanecarboxamido] butane; Pierce) for one hour at 4°C. After washing to remove residual Btn-BMCC, the labeled proteins were separated by SDS-PAGE and transferred to nitrocellulose membranes. Blots were probed with streptavidin-conjugated horseradish peroxidase (HRP) and the labeled proteins detected with Enhanced Chemiluminescence (ECL; Amersham).

Immuno-EM procedure

Neurons were fixed in 4% formaldehyde, 1% glutaraldehyde in PBS for 15-20 min at 37°C. All further steps were done using rapid microwave irradiation to accelerate sample processing (PELCO 3451; Ted Pella). Fixed cells were washed in PBS, quenched with 50 mM glycine and permeabilized with 0.1% saponin in PBS for 30 sec at room temperature. Following incubation in blocking solution (1% NGS, 1% BSA, 0.1% fish gelatin; Aurion), coverslips were incubated

with primary antibody (monoclonal anti-EGFP, 1:200; Roche, No. 1181446) in blocking solution, washed with PBS, and incubated with secondary antibody (1:40; Fluoro-nanogold, Nanoprobes) in PBS-BSA. After rinsing with PBS-BSA, cells were again fixed in 2% glutaraldehyde in PBS, washed with PBS, and quenched with 50 mM glycine. Following washes in PBS-BSA and $H_2O$, gold particles were silver enhanced (Nanoprobes HQ kit) for 4-5 min, washed in $H_2O$ and postfixed in 0.1% $OsO_4$, 0.8% potassium ferricyanide in 0.1 M cacodylate buffer. Cells were then dehydrated with ascending alcohol series (50%, 70%, 95%, 3 x 100%) and coverslips embedded in resin (Embed 812, EMS). After polymerizing overnight at 60°C, excess resin was removed and coverslips were dissolved in hydrofluoric acid. Following ~30 min of rinsing in water, resin-embedded neurons were dried and small fragments of resin mounted onto blocks and sectioned by ultramicrotome. Sections were collected on copper grids, post-stained in uranyl acetate and lead citrate prior to image acquisition.

## Figures and Tables

**Figure S1.** Relative expression levels of α– and βSAP97 in hippocampal neurons.
(A) Western blots of lysates from control neurons or those infected with α– or βSAP97-EGFP, probed with antibodies against SAP97 (top panel), GFP (middle panel), or tubulin (bottom panel). Arrowheads indicate endogenous SAP97 as well as EGFP-tagged α– and β-isoforms. (B) Left column: Images depicting the levels of PSD-95 immunostaining (middle panel; red) in untransfected and PSD-95-EGFP-transfected (top; green) hippocampal neurons. The graph below shows the PSD-95 level in cells expressing PSD-95-EGFP relative to untransfected cells. Note the lack of PSD-95-EGFP overexpression in transfected neurons. Right: Images demonstrating the relative expression levels of transfected PSD-95-EGFP (top), αSAP97-EGFP (middle), and βSAP97-EGFP (bottom). The bar graph shows the levels of overexpression of transfected α– and βSAP97-EGFP relative to PSD-95-EGFP.

**Figure S2.** Subcellular localization of α–, β– and ΔSAP97.
(A) Intensities of SAP97-EGFP puncta in dendritic spines of lentivirus-infected neurons. αSAP97-EGFP puncta have higher fluorescence intensities than β- or ΔSAP97-EGFP puncta. Mean ± SEM spine intensities from $n \geq 11$ neurons for each construct. (B) Spine/shaft ratios of SAP97-EGFP constructs in hippocampal neurons. αSAP97-EGFP puncta have higher enrichment in spines relative to dendritic shafts compared to β- or ΔSAP97-EGFP (mean ± SEM, $n \geq 11$ neurons per construct). (C) ΔSAP97-GFP localizes to active synapses as determined by loading of synaptic vesicles with the styryl dye FM4-64.

**Figure S3.** Effects of latrunculin A on actin and SAP97.
(A) Images showing the effect of acute (5 min, 5 μM) latrunculin A treatment on EGFP-β-actin (left panels, green) and F-actin (middle, red). Neurons expressing EGFP-β-actin (green) were incubated in Tyrode solution in the absence (control, top) or presence (bottom images) of 5 μM latrunculin A for 5 min, fixed and labeled with Alexa 568-phalloidin (red). The treatment disrupts the actin cytoskeleton, as judged by the diffuse appearance of GFP fluorescence as well as the reduction in F-actin staining. (B) Bar graph depicting the relative intensities of synaptic SAP97-EGFP puncta after 15 min latrunculin A treatment (5 μM in Tyrode solution). Intensities were

quantified in live neurons expressing α-, β- or ΔSAP97-GFP and normalized to pre-treatment levels. Data are shown as means ± SEM (n ≥ 25 puncta from 3 cells for each construct). (C) Images showing the effects of longer-term (5 h, 10 μM) latrunculin A treatment on βSAP97-EGFP (left panels, green) and F-actin (middle panels, red). Neurons expressing βSAP97-EGFP were incubated for 5 h in the absence or presence of 10 μM latrunculin A (added to the medium), then fixed and stained with Alexa 568-labeled phalloidin. This treatment disrupts most of the actin cytoskeleton and βSAP97-EGFP localization, as evidenced by the absence of dendritic spines or prominent βSAP97-EGFP puncta.

**Figure S4.** Subsynaptic localization of α– and βSAP97-EGFP.

(A) EM micrographs depicting the PSD localization of αSAP97-EGFP. Note the prominent silver-enhanced immunogold labeling associated with postsynaptic densities. White arrowheads denote the PSD, black arrows point to immunogold labeling.

(B) EM micrographs showing the most common sites of βSAP97-EGFP labeling within dendritic spines. Labeling is often seen adjacent to the PSD, either associated with the plasma membrane or at presumed intracellular locations within the spine head (top panels and lower left). Occasionally, labeling was also observed at the PSD or within presynaptic boutons (lower right panel).

**Figure S5.** Specificity of interaction between SAP97 isoforms and GluR1.

(A) Western blot of HEK cell lysates from cells cotransfected with mCh-GluR1 and α-, β- or ΔSAP97-EGFP. Cell lysates were separated by SDS-PAGE and probed for the expression of the SAP97 constructs using a polyclonal rabbit anti-GFP antibody. (B) Western blot of immunoprecipitated material from HEK cell lysates. Lysates were immunoprecipitated with IgG antibody (as control) or polyclonal rabbit anti-RFP, separated by SDS-PAGE, and probed for co-immunoprecipitation of the SAP97-EGFP fusion proteins using monoclonal anti-GFP antibody. (C) Images of dendrites from neurons transfected with α- or βSAP97-EGFP (green; left panels) and stained with antibodies against endogenous GluR1 (red; top images) or GluR3 (red; bottom). Both SAP97 isoforms cause the accumulation of GluR1 within dendritic spines but have no effect on GluR3 localization.

**Figure S6.** Fluorescence recovery of mCh-GluR1 after antibody crosslinking.
(A) Average intensities of SAP97-EGFP puncta in dendritic spines of calcium phosphate-transfected neurons. Similar to lentivirus-infected neurons (Fig. S2A), αSAP97-EGFP puncta in transfected neurons have higher fluorescence intensities than β- and ΔSAP97-EGFP puncta (mean ± SEM, n ≥ 54 puncta from 8 neurons per construct). (B) FRAP of mCh-GluR1 (red; indicated by arrowheads) in spines of neurons coexpressing βSAP97-EGFP (green; left panels). Upper panels depict the recovery under normal conditions, while the lower images show the recovery following crosslinking of surface mCh-GluR1 using sequential incubation with polyclonal RFP primary antibodies and anti-rabbit secondary antibodies. The quantification of these data is shown in Fig. 5H. In addition to abolishing mCh-GluR1 recovery, antibody crosslinking also changes the distribution of the receptors in dendrites, creating clusters of linked receptor subunits.

**Figure S7.** Kinetic and biochemical properties of EGFP-tagged α– and βSAP97 in the absence of PSD-95.
(A) Fluorescence recovery of αSAP97-EGFP+sh95 (gray) and EGFP-βSAP97+sh95 (black) compared to those of αSAP97-EGFP and EGFP-βSAP97 alone (dashed lines). Note that the loss of PSD-95 in infected neurons does not alter the exchange kinetics of either SAP97 isoform. (B) Average fluorescence intensity of puncta of EGFP-βSAP97 +/- sh95 after Triton extraction relative to the initial intensity. Again, loss of PSD-95 does not affect the Triton extractability of EGFP-βSAP97. (C) Images of neurons expressing EGFP-βSAP97+sh95 under control conditions or following latrunculin A treatment, demonstrating that PSD-95 knockdown does not affect the latrunculin A sensitivity of EGFP-βSAP97 (compare with Fig. S3C).

**Figure S8.** Transsynaptic signaling effects of SAP97 isoforms.
(A) Neurons were transfected with α– (green; left), β– (center) or ΔSAP97-EGFP (right) and loaded with FM4-64 (red) to label presynaptic boutons. Arrows in the magnified image segments indicate sites where presynaptic FM4-64 puncta are adjacent to postsynaptic SAP97-EGFP; arrowheads indicate control FM4-64 puncta (adjacent to untransfected neurons). Scale bars = 15 μm. (B) Cumulative probability histograms plotting the intensities of FM4-64 puncta adjacent to postsynaptic α– (left), β- (center) or ΔSAP97-EGFP (right; black solid lines) compared to

untransfected neurons in the same fields of view (dashed lines). Note that the intensities of puncta apposed to α– and βSAP97 are shifted to the right (i.e. more intense) compared with control puncta, while those apposed to ΔSAP97 are indistinguishable from control puncta. (C) Quantification of the data shown in B. Average intensities for FM4-64 puncta apposed to postsynaptic α–, β– or ΔSAP97-EGFP are expressed relative to control puncta in the same fields of view (indicated by the black line at 1). Note that both α– and βSAP97 significantly increase FM4-64 puncta intensity compared to ΔSAP97 and untransfected cells ($p<0.0005$, t test, mean ± SEM from $n \geq 8$ fields of view). (D,E) FM4-64 destaining curves of puncta adjacent to α– or βSAP97-EGFP (black) compared to untransfected neurons in the same fields of view (gray). Note that puncta adjacent to α– or βSAP97-EGFP destain at similar rates to control puncta (mean intensity values ± SEM for $n = 2$ fields of view for αSAP97 and 3 fields for βSAP97; $n \geq 120$ puncta per condition).

# Figure S1; Waites *et al.*

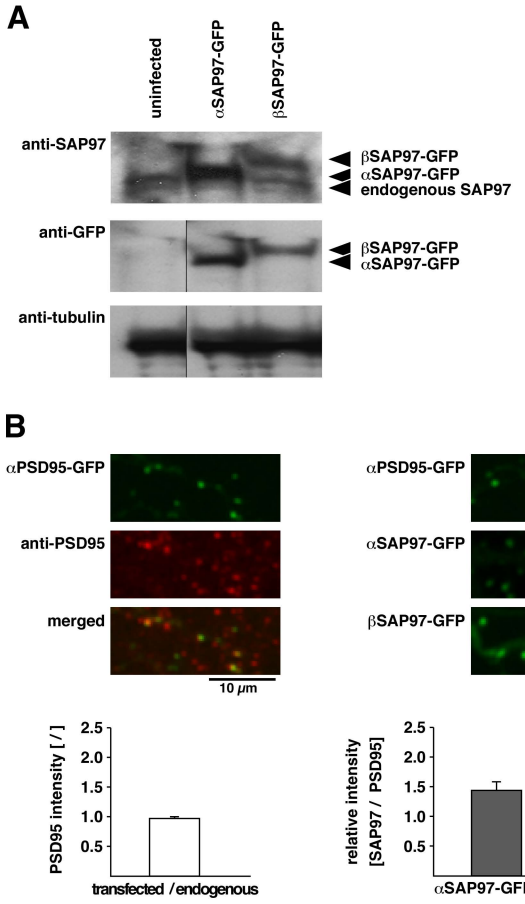

# Figure S2; Waites *et al.*

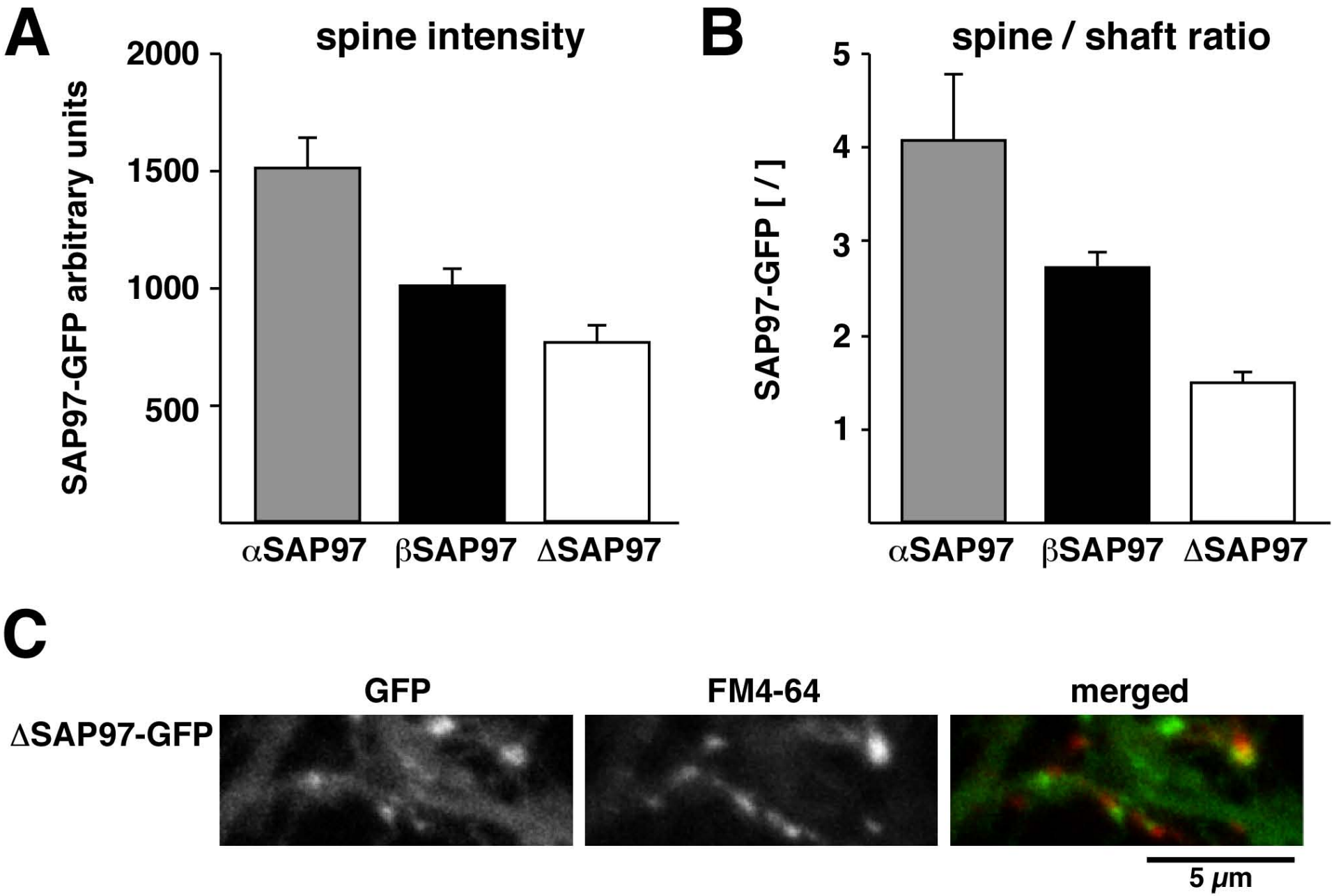

# Figure S3; Waites *et al.*

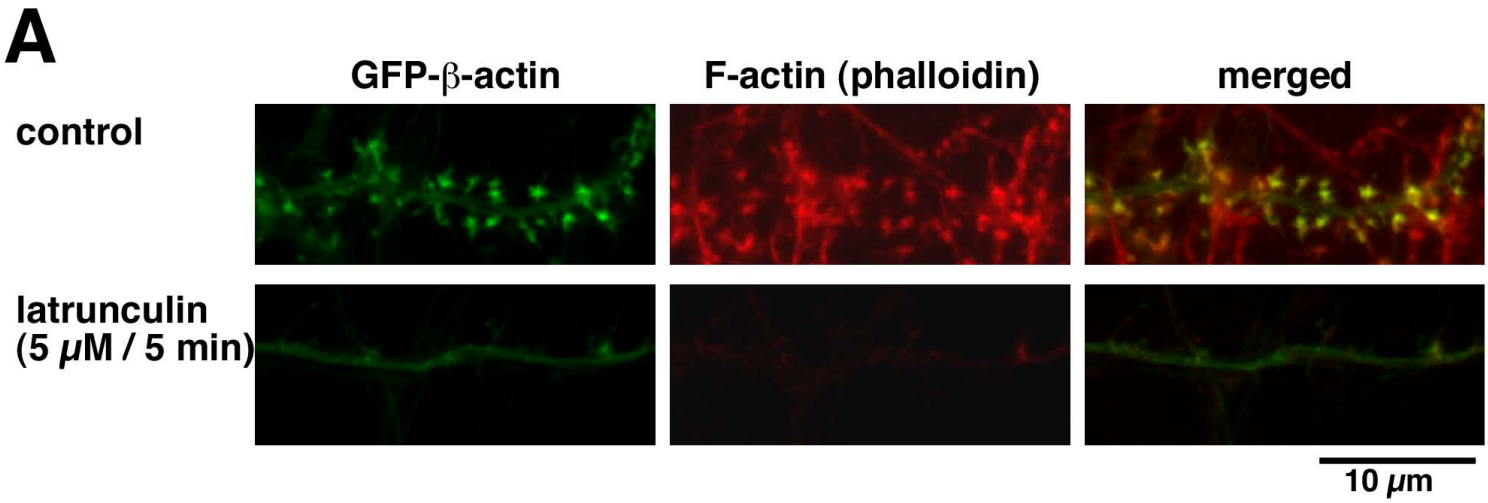


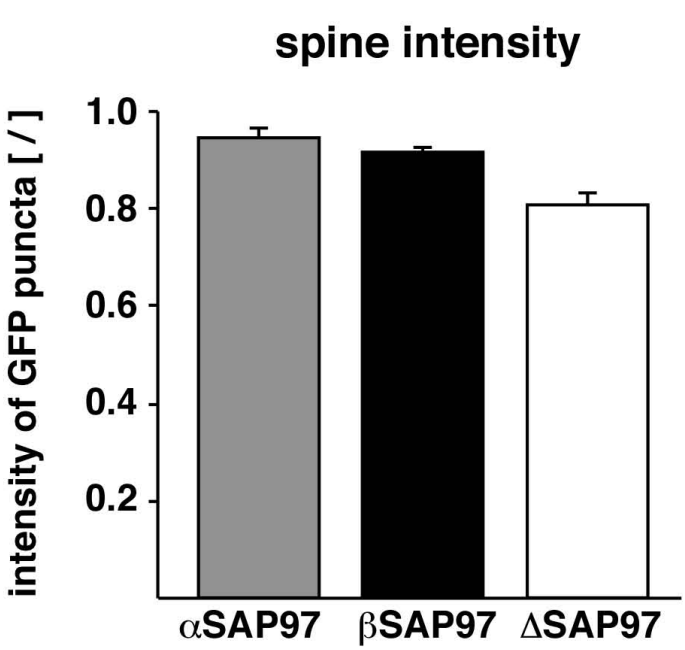


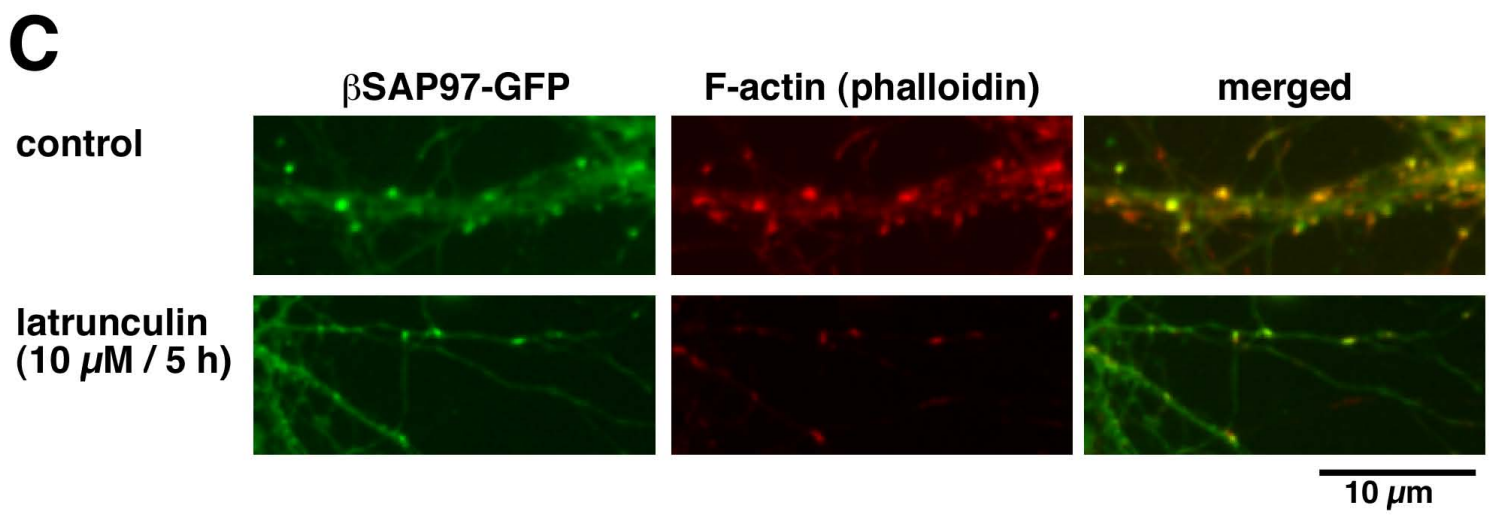

# Figure S4; Waites *et al.*

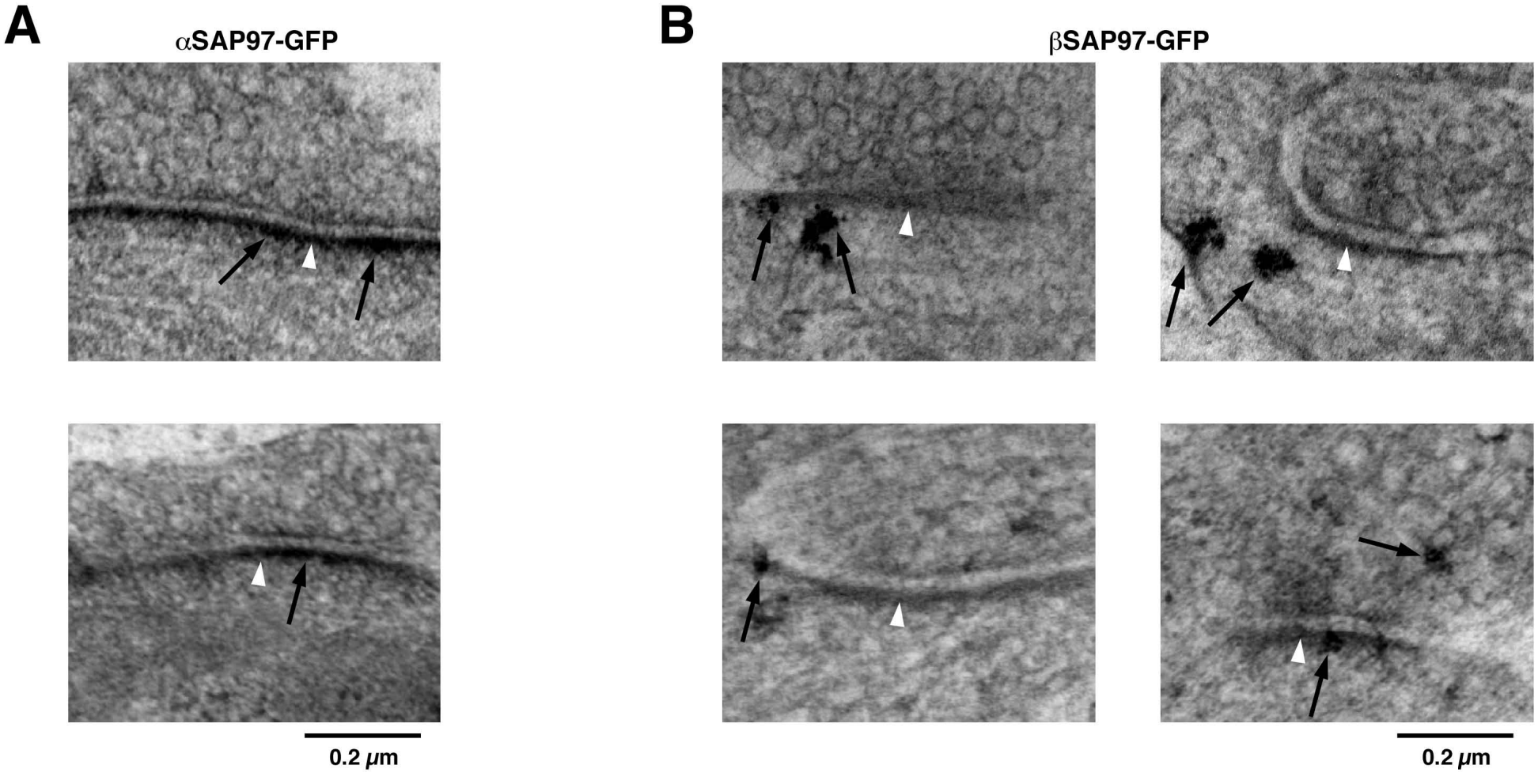

# Figure S5; Waites *et al.*

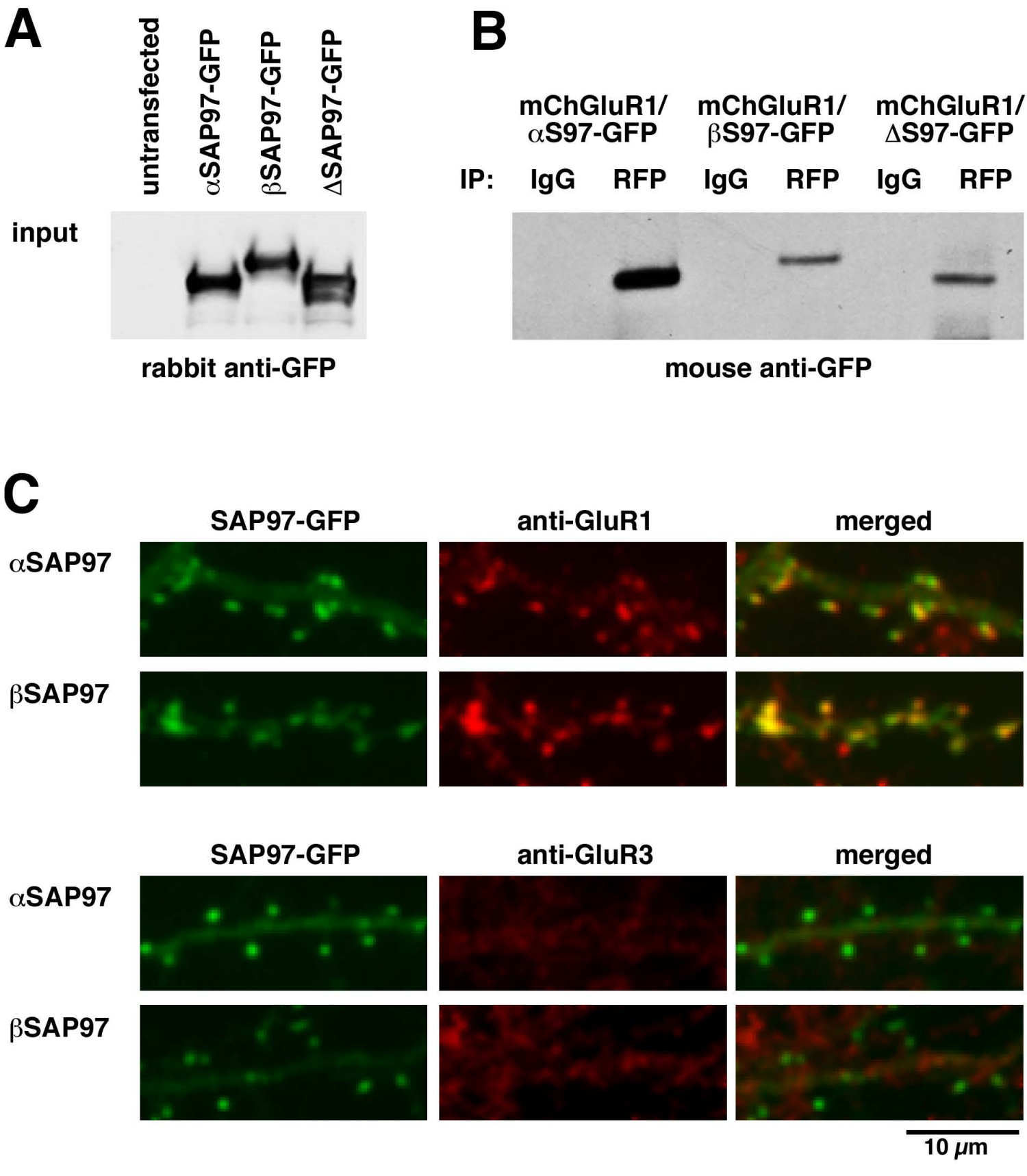

# Figure S6; Waites *et al.*

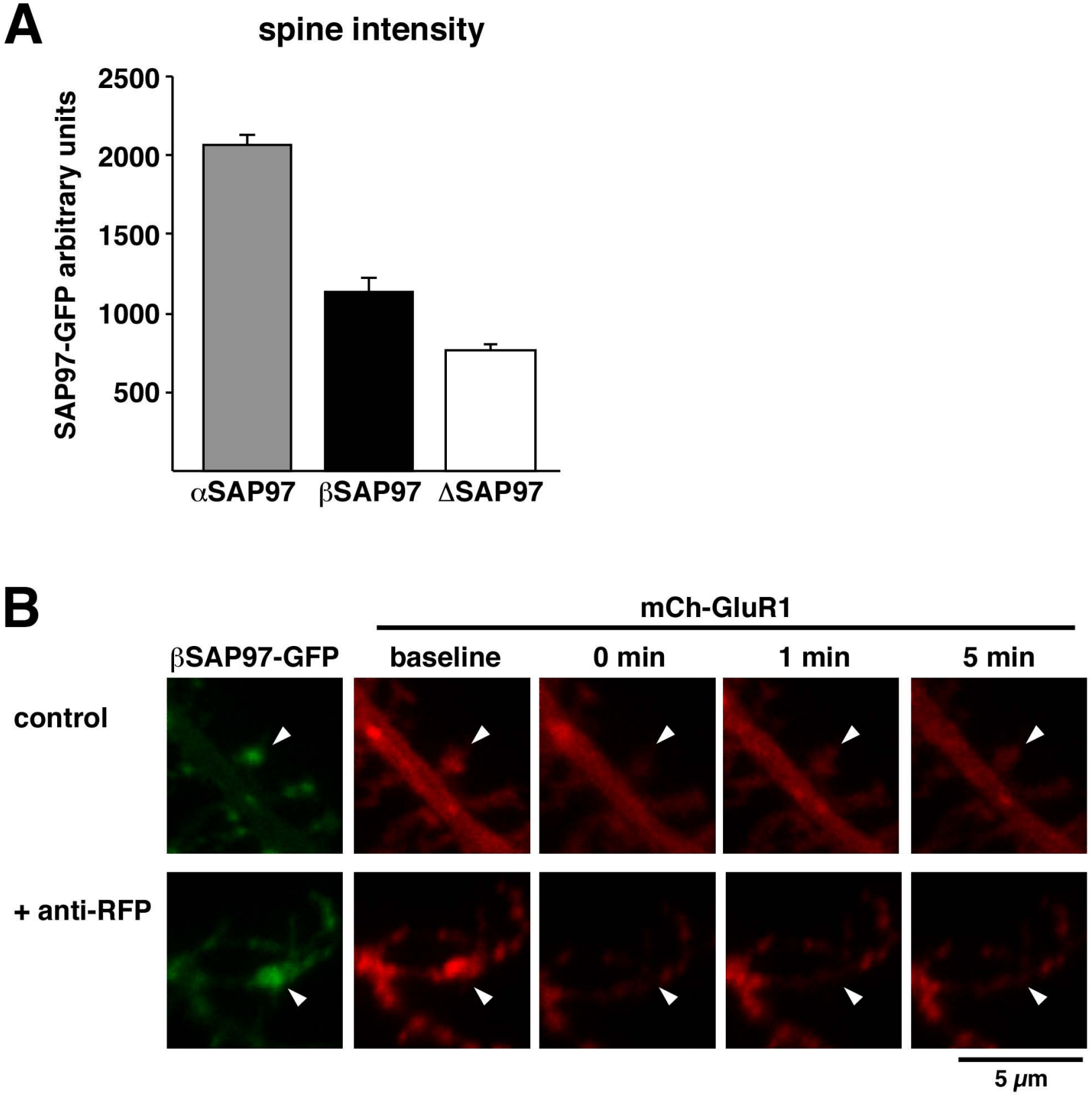

# Figure S7; Waites *et al.*

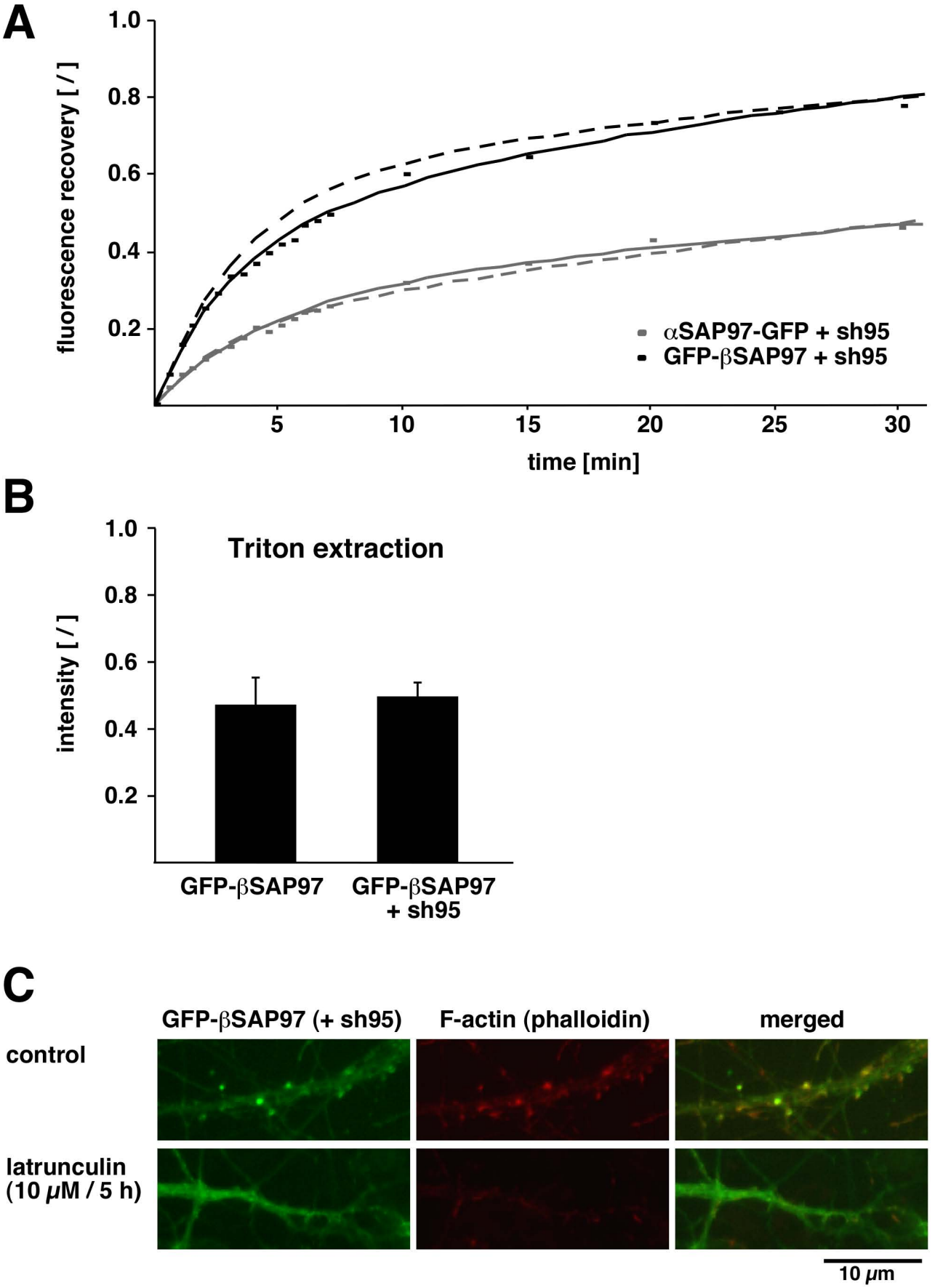

Figure S8; Waites *et al.*

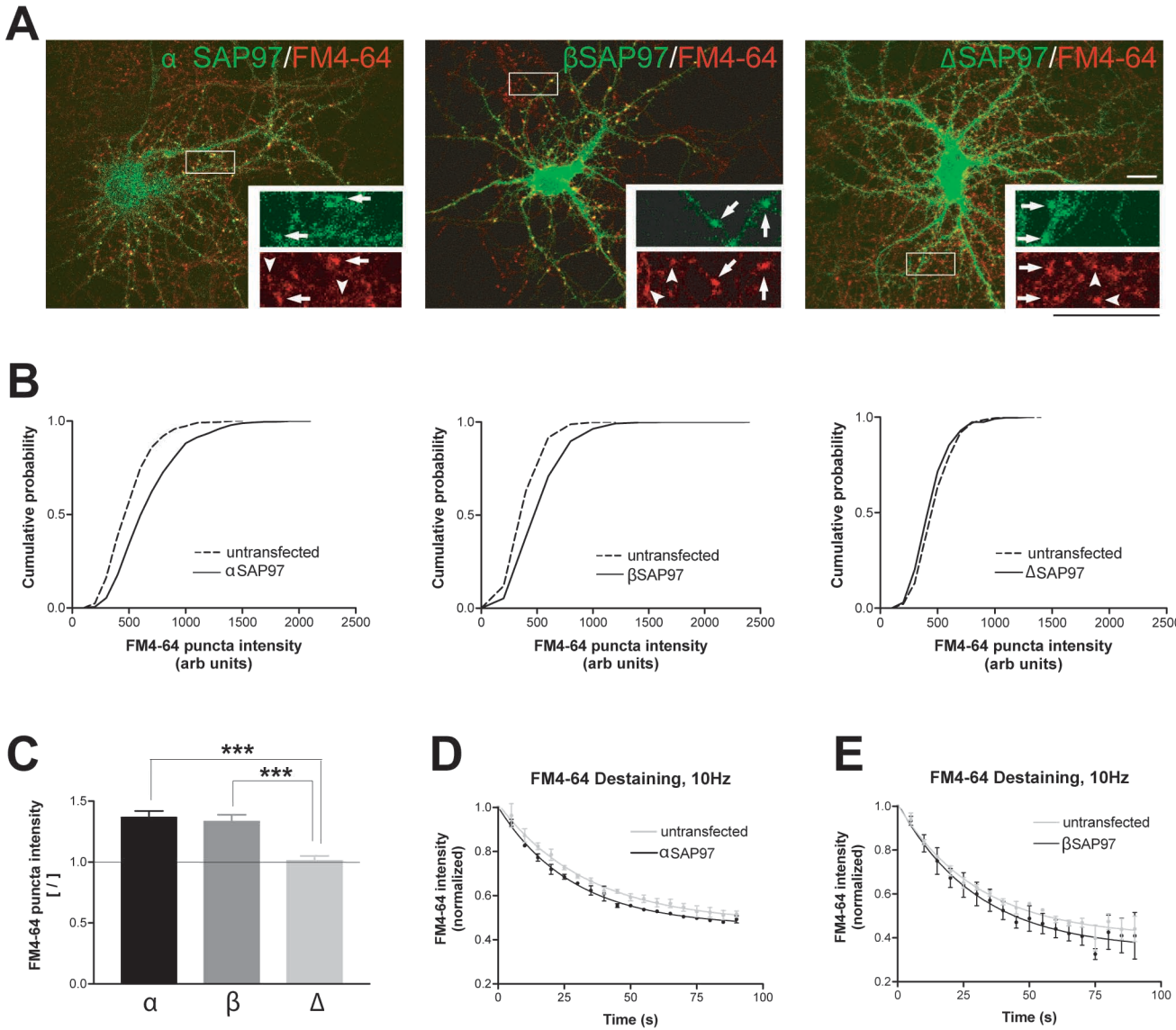

Supplementary table S1: Summary of FRAP data, including timepoints [min], mean fluorescence recovery [ / ], standard deviation [ / ] and number of data points.

| | αSAP97-GFP, lentivirus | | | βSAP97-GFP, lentivirus | | | ΔSAP97-GFP, lentivirus | | | αSAP97-GFP + 2-br-palmitate, lentiv. | | | βSAP97-GFP + 2-br-palmitate, lentiv. | | | αSAP97-GFP (+ sh95), lentivirus | | | GFP-βSAP97 (+ sh95), lentivirus | | |
|---|---|---|---|---|---|---|---|---|---|---|---|---|---|---|---|---|---|---|---|---|---|
| time [min] | mean | SD | n | mean | SD | n | mean | SD | n | mean | SD | n | mean | SD | n | mean | SD | n | mean | SD | n |
| 0 | 0.00 | 0.00 | 25 | 0.00 | 0.00 | 22 | 0.00 | 0.00 | 26 | 0.00 | 0.00 | 23 | 0.00 | 0.00 | 29 | 0.00 | 0.00 | 10 | 0.00 | 0.00 | 22 |
| 0.5 | 0.05 | 0.03 | 25 | 0.17 | 0.07 | 22 | 0.42 | 0.13 | 26 | 0.21 | 0.12 | 23 | 0.16 | 0.07 | 27 | 0.05 | 0.02 | 10 | 0.08 | 0.05 | 22 |
| 1 | 0.08 | 0.05 | 25 | 0.24 | 0.09 | 22 | 0.60 | 0.13 | 26 | 0.30 | 0.15 | 23 | 0.23 | 0.12 | 28 | 0.08 | 0.04 | 10 | 0.16 | 0.08 | 22 |
| 1.5 | 0.10 | 0.05 | 25 | 0.31 | 0.12 | 22 | 0.70 | 0.18 | 26 | 0.36 | 0.17 | 23 | 0.28 | 0.12 | 28 | 0.10 | 0.03 | 10 | 0.21 | 0.08 | 22 |
| 2 | 0.12 | 0.05 | 25 | 0.37 | 0.13 | 22 | 0.73 | 0.16 | 26 | 0.38 | 0.14 | 23 | 0.32 | 0.12 | 28 | 0.12 | 0.03 | 10 | 0.25 | 0.09 | 22 |
| 2.5 | 0.15 | 0.07 | 25 | 0.42 | 0.14 | 22 | 0.79 | 0.15 | 26 | 0.43 | 0.18 | 23 | 0.35 | 0.13 | 29 | 0.14 | 0.05 | 10 | 0.29 | 0.10 | 22 |
| 3 | 0.16 | 0.07 | 25 | 0.46 | 0.15 | 22 | 0.78 | 0.19 | 26 | 0.47 | 0.19 | 23 | 0.38 | 0.16 | 29 | 0.15 | 0.04 | 10 | 0.33 | 0.10 | 22 |
| 3.5 | 0.17 | 0.07 | 25 | 0.50 | 0.16 | 22 | 0.79 | 0.18 | 26 | 0.47 | 0.18 | 23 | 0.41 | 0.15 | 29 | 0.17 | 0.07 | 10 | 0.34 | 0.10 | 22 |
| 4 | 0.20 | 0.08 | 25 | 0.53 | 0.17 | 22 | 0.81 | 0.20 | 26 | 0.48 | 0.18 | 23 | 0.44 | 0.17 | 29 | 0.20 | 0.04 | 10 | 0.36 | 0.09 | 22 |
| 4.5 | 0.19 | 0.06 | 25 | 0.56 | 0.16 | 22 | 0.82 | 0.16 | 26 | 0.52 | 0.18 | 23 | 0.45 | 0.17 | 29 | 0.19 | 0.05 | 10 | 0.39 | 0.09 | 22 |
| 5 | 0.22 | 0.06 | 23 | 0.56 | 0.16 | 22 | 0.86 | 0.18 | 26 | 0.54 | 0.19 | 23 | 0.49 | 0.19 | 29 | 0.21 | 0.07 | 10 | 0.42 | 0.10 | 22 |
| 5.5 | 0.23 | 0.05 | 23 | 0.58 | 0.18 | 22 | 0.85 | 0.18 | 26 | 0.55 | 0.20 | 23 | 0.51 | 0.18 | 29 | 0.22 | 0.08 | 10 | 0.43 | 0.10 | 22 |
| 6 | 0.23 | 0.06 | 23 | 0.63 | 0.20 | 22 | 0.85 | 0.16 | 26 | 0.55 | 0.18 | 23 | 0.52 | 0.19 | 29 | 0.24 | 0.08 | 10 | 0.46 | 0.10 | 22 |
| 6.5 | 0.25 | 0.06 | 23 | 0.63 | 0.19 | 22 | 0.86 | 0.18 | 26 | 0.57 | 0.19 | 23 | 0.53 | 0.19 | 29 | 0.25 | 0.07 | 10 | 0.48 | 0.11 | 22 |
| 7 | 0.25 | 0.06 | 20 | 0.66 | 0.19 | 22 | 0.85 | 0.16 | 23 | 0.61 | 0.27 | 23 | 0.53 | 0.19 | 29 | 0.26 | 0.06 | 10 | 0.49 | 0.13 | 22 |
| 10 | 0.31 | 0.08 | 21 | 0.68 | 0.20 | 20 | 0.91 | 0.13 | 23 | | | | 0.62 | 0.22 | 29 | 0.32 | 0.08 | 9 | 0.60 | 0.14 | 14 |
| 15 | 0.35 | 0.09 | 18 | 0.73 | 0.21 | 20 | 0.92 | 0.16 | 22 | | | | 0.66 | 0.20 | 28 | 0.37 | 0.10 | 9 | 0.64 | 0.15 | 22 |
| 20 | 0.40 | 0.10 | 18 | 0.78 | 0.19 | 20 | 0.97 | 0.19 | 18 | | | | 0.69 | 0.20 | 28 | 0.43 | 0.09 | 9 | 0.73 | 0.18 | 22 |
| 25 | 0.44 | 0.09 | 18 | 0.80 | 0.23 | 20 | 0.96 | 0.16 | 17 | | | | 0.70 | 0.20 | 27 | 0.43 | 0.08 | 9 | 0.76 | 0.20 | 22 |
| 30 | 0.47 | 0.10 | 18 | 0.81 | 0.13 | 18 | 0.96 | 0.21 | 13 | | | | 0.71 | 0.19 | 28 | 0.46 | 0.05 | 9 | 0.78 | 0.17 | 22 |

| | αSAP97-GFP (+ mCh-GluR1) | | | βSAP97-GFP (+ mCh-GluR1) | | | ΔSAP97-GFP (+ mCh-GluR1) | | |
|---|---|---|---|---|---|---|---|---|---|
| time [min] | mean | SD | n | mean | SD | n | mean | SD | n |
| 0 | 0.00 | 0.00 | 16 | 0.00 | 0.00 | 14 | 0.00 | 0.00 | 12 |
| 0.5 | 0.10 | 0.04 | 16 | 0.13 | 0.07 | 14 | 0.49 | 0.19 | 12 |
| 1 | 0.16 | 0.05 | 16 | 0.24 | 0.12 | 14 | 0.73 | 0.24 | 12 |
| 1.5 | 0.20 | 0.07 | 16 | 0.29 | 0.12 | 14 | 0.74 | 0.22 | 12 |
| 2 | 0.23 | 0.07 | 16 | 0.37 | 0.15 | 14 | 0.83 | 0.20 | 12 |
| 2.5 | 0.24 | 0.07 | 16 | 0.44 | 0.15 | 14 | 0.86 | 0.24 | 12 |
| 3 | 0.26 | 0.08 | 16 | 0.48 | 0.18 | 14 | 0.91 | 0.26 | 12 |
| 3.5 | 0.28 | 0.09 | 16 | 0.51 | 0.17 | 14 | 0.92 | 0.27 | 12 |
| 4 | 0.28 | 0.09 | 16 | 0.55 | 0.18 | 14 | 0.89 | 0.24 | 12 |
| 4.5 | 0.31 | 0.09 | 16 | 0.56 | 0.17 | 14 | 0.85 | 0.22 | 12 |
| 5 | 0.31 | 0.09 | 16 | 0.59 | 0.16 | 14 | 0.82 | 0.24 | 12 |
| 5.5 | 0.33 | 0.10 | 15 | 0.63 | 0.18 | 14 | 0.85 | 0.26 | 12 |
| 6 | 0.33 | 0.10 | 15 | 0.65 | 0.17 | 14 | 0.91 | 0.32 | 12 |
| 6.5 | 0.34 | 0.10 | 15 | 0.67 | 0.16 | 14 | 0.96 | 0.30 | 12 |
| 7 | 0.35 | 0.10 | 15 | 0.66 | 0.16 | 14 | 0.93 | 0.34 | 9 |
| 10 | 0.39 | 0.10 | 15 | 0.75 | 0.15 | 14 | | | |
| 15 | 0.44 | 0.11 | 15 | 0.83 | 0.16 | 14 | | | |
| 20 | 0.50 | 0.12 | 15 | 0.91 | 0.10 | 14 | | | |
| 25 | 0.51 | 0.13 | 15 | 0.96 | 0.16 | 12 | | | |
| 30 | 0.55 | 0.12 | 14 | 0.98 | 0.22 | 9 | | | |

| | βSAP97-GFP (+ mCh-GluR1) | | | βSAP97-GFP (+ mCh-GluR1), anti-RFP | | | βSAP97-GFP, anti-GluR1 (endogenous) | | |
|---|---|---|---|---|---|---|---|---|---|
| time [min] | mean | SD | n | mean | SD | n | mean | SD | n |
| 0 | 0.00 | 0.00 | 17 | 0.00 | 0.00 | 22 | 0.00 | 0.00 | 14 |
| 0.5 | 0.11 | 0.05 | 17 | 0.09 | 0.04 | 19 | 0.10 | 0.06 | 14 |
| 1 | 0.18 | 0.08 | 17 | 0.13 | 0.08 | 22 | 0.17 | 0.08 | 14 |
| 1.5 | 0.23 | 0.11 | 16 | 0.19 | 0.08 | 21 | 0.21 | 0.09 | 14 |
| 2 | 0.27 | 0.12 | 16 | 0.24 | 0.11 | 22 | 0.26 | 0.10 | 14 |
| 2.5 | 0.30 | 0.14 | 17 | 0.26 | 0.09 | 22 | 0.29 | 0.12 | 14 |
| 3 | 0.32 | 0.13 | 17 | 0.28 | 0.11 | 22 | 0.37 | 0.15 | 14 |
| 3.5 | 0.38 | 0.15 | 16 | 0.31 | 0.11 | 22 | 0.38 | 0.14 | 14 |
| 4 | 0.40 | 0.13 | 17 | 0.33 | 0.11 | 21 | 0.42 | 0.15 | 14 |
| 4.5 | 0.43 | 0.14 | 17 | 0.35 | 0.12 | 22 | 0.43 | 0.15 | 14 |
| 5 | 0.43 | 0.14 | 17 | 0.37 | 0.12 | 22 | 0.47 | 0.16 | 14 |
| 5.5 | 0.44 | 0.14 | 17 | 0.39 | 0.14 | 22 | 0.50 | 0.16 | 14 |
| 6 | 0.48 | 0.14 | 17 | 0.42 | 0.15 | 22 | 0.53 | 0.17 | 14 |
| 6.5 | 0.49 | 0.11 | 17 | 0.41 | 0.13 | 22 | 0.56 | 0.17 | 14 |
| 7 | 0.52 | 0.13 | 17 | 0.44 | 0.16 | 22 | 0.60 | 0.17 | 5 |
| 10 | 0.60 | 0.15 | 12 | 0.50 | 0.16 | 21 | 0.77 | 0.18 | 5 |
| 15 | 0.65 | 0.14 | 12 | 0.56 | 0.19 | 21 | 0.84 | 0.13 | 5 |
| 20 | 0.72 | 0.18 | 10 | 0.65 | 0.18 | 19 | 0.85 | 0.10 | 5 |
| 25 | 0.71 | 0.12 | 10 | 0.71 | 0.20 | 12 | 0.87 | 0.16 | 2 |
| 30 | 0.79 | 0.16 | 10 | 0.72 | 0.18 | 13 | 0.85 | 0.10 | 2 |

| | mCh-GluR1 (+ αSAP97-GFP) | | | mCh-GluR1 (+ βSAP97-GFP) | | | mCh-GluR1 (+ ΔSAP97-GFP) | | | mCh-GluR1 (+ soluble GFP) | | | mCh-GluR1 (+ αSAP97-GFP), anti-RFP | | | mCh-GluR1 (+ βSAP97-GFP), anti-RFP | | |
|---|---|---|---|---|---|---|---|---|---|---|---|---|---|---|---|---|---|---|
| time [min] | mean | SD | n | mean | SD | n | mean | SD | n | mean | SD | n | mean | SD | n | mean | SD | n |
| 0 | 0.00 | 0.00 | 33 | 0.00 | 0.00 | 33 | 0.00 | 0.00 | 14 | 0.00 | 0.00 | 8 | 0.00 | 0.00 | 8 | 0.00 | 0.00 | 10 |
| 0.5 | 0.11 | 0.08 | 17 | 0.21 | 0.11 | 18 | | | | | | | -0.02 | 0.03 | 4 | -0.05 | 0.09 | 4 |
| 1 | 0.22 | 0.10 | 33 | 0.30 | 0.17 | 32 | 0.43 | 0.16 | 13 | 0.54 | 0.15 | 8 | 0.00 | 0.06 | 8 | 0.01 | 0.11 | 10 |
| 1.5 | 0.21 | 0.14 | 17 | 0.36 | 0.16 | 18 | | | | | | | -0.02 | 0.04 | 4 | -0.01 | 0.08 | 4 |
| 2 | 0.29 | 0.11 | 33 | 0.43 | 0.20 | 33 | 0.56 | 0.15 | 14 | 0.69 | 0.23 | 8 | 0.01 | 0.04 | 8 | 0.01 | 0.16 | 10 |
| 2.5 | 0.33 | 0.14 | 17 | 0.52 | 0.19 | 18 | | | | | | | -0.02 | 0.03 | 4 | -0.05 | 0.15 | 4 |
| 3 | 0.38 | 0.11 | 33 | 0.51 | 0.18 | 33 | 0.67 | 0.13 | 13 | 0.75 | 0.15 | 8 | 0.01 | 0.05 | 8 | 0.03 | 0.08 | 10 |
| 3.5 | 0.36 | 0.15 | 17 | 0.55 | 0.19 | 18 | | | | | | | 0.00 | 0.01 | 4 | -0.04 | 0.13 | 4 |
| 4 | 0.42 | 0.14 | 33 | 0.58 | 0.20 | 33 | 0.72 | 0.19 | 13 | 0.70 | 0.26 | 8 | 0.02 | 0.06 | 8 | 0.06 | 0.15 | 10 |
| 4.5 | 0.42 | 0.19 | 17 | 0.61 | 0.20 | 18 | | | | | | | 0.00 | 0.02 | 4 | 0.01 | 0.03 | 4 |
| 5 | 0.44 | 0.16 | 33 | 0.61 | 0.20 | 33 | 0.71 | 0.15 | 13 | 0.82 | 0.30 | 8 | 0.05 | 0.04 | 8 | 0.06 | 0.08 | 9 |
| 5.5 | 0.46 | 0.17 | 17 | 0.64 | 0.18 | 18 | | | | | | | 0.02 | 0.03 | 4 | 0.02 | 0.06 | 4 |
| 6 | 0.48 | 0.14 | 33 | 0.63 | 0.18 | 32 | 0.73 | 0.15 | 14 | 0.78 | 0.26 | 7 | 0.04 | 0.04 | 8 | 0.08 | 0.07 | 9 |
| 6.5 | 0.45 | 0.17 | 16 | 0.62 | 0.16 | 16 | | | | | | | 0.02 | 0.03 | 4 | 0.05 | 0.08 | 4 |
| 7 | 0.51 | 0.13 | 26 | 0.64 | 0.19 | 18 | 0.83 | 0.06 | 4 | 0.85 | 0.19 | 7 | 0.04 | 0.06 | 8 | 0.10 | 0.10 | 8 |
| 10 | 0.62 | 0.16 | 16 | 0.72 | 0.24 | 15 | 0.84 | 0.20 | 12 | | | | 0.06 | 0.08 | 8 | 0.12 | 0.14 | 10 |
| 15 | 0.63 | 0.16 | 16 | 0.72 | 0.21 | 15 | 0.82 | 0.24 | 12 | | | | 0.10 | 0.09 | 8 | 0.16 | 0.16 | 10 |
| 20 | 0.71 | 0.16 | 16 | 0.90 | 0.22 | 15 | 0.82 | 0.14 | 11 | | | | 0.11 | 0.09 | 8 | 0.18 | 0.11 | 8 |
| 25 | 0.75 | 0.17 | 15 | 0.86 | 0.22 | 15 | 0.88 | 0.25 | 11 | | | | 0.11 | 0.11 | 8 | 0.23 | 0.16 | 7 |
| 30 | 0.77 | 0.12 | 15 | 0.77 | 0.28 | 12 | 0.93 | 0.35 | 10 | | | | 0.17 | 0.16 | 6 | 0.19 | 0.17 | 8 |

| | mEPSC amplitude [pA] | mEPSC frequency [Hz] | Evoked EPSC amplitude [pA] |
|---|---|---|---|
| **control** | 15.3 ± 0.27 | 1.20 ± 0.25 | 256 ± 40 |
| **αSAP97-GFP** | 18.4 ± 0.70** | 1.63 ± 0.38 | 472 ± 128*** |
| **βSAP97-GFP** | 13.7 ± 0.17** | 0.29 ± 0.09* | 87 ± 17* |
| **ΔSAP97-GFP** | 16.0 ± 0.34 | 1.23 ± 0.54 | |

Supplementary Table S2
Summary of miniature and evoked EPSC data for SAP97 isoforms.

Pyramidal neurons (DIV11-14) were transfected 24-48 h prior to mEPSC recording with SAP97 constructs (or GFP for control). Paired whole cell evoked EPSCs were recorded from α and βSAP97-expressing neurons and untransfected controls. Data are shown as means ± SEM; asterisks denote values that are statistically significant (* $p < 0.01$, ** $p < 0.001$, *** $p < 0.05$); $n > 400$ mEPSC events from ≥ 5 cells for each condition; $n \geq 10$ cells with ≥ 90 EPSCs per cell.